fermentation

MDPI

Article

Deep Eutectic Solvent Pretreatment of Water Hyacinth for Improved Holocellulosic Saccharification and Fermentative Co-Production of Xylitol and Lipids Using *Rhodosporidium toruloides* NCIM 3547

Ramachandran Devasena Umai [1], Samuel Jacob [1,*] and Vinod Kumar [2,*]

[1] Department of Biotechnology, School of Bioengineering, College of Engineering and Technology, Faculty of Engineering and Technology, SRM Institute of Science and Technology, Kattankulathur 603203, Tamil Nadu, India
[2] School of Water, Energy and Environment, Cranfield University, Cranfield MK43 0AL, UK
* Correspondence: samueljb@srmist.edu.in (S.J.); Vinod.Kumar@cranfield.ac.uk (V.K.)

Abstract: In this study, delignification of water hyacinth (WH) using a mild ionic liquid-like chemical deep eutectic solvent (DES) synthesized using choline chloride and urea was conducted and the process parameters were optimized by Box–Behnken design (BBD)-based response surface methodology (RSM). From the results, a delignification of 64.32 ± 4.08% (*w*/*w*) was obtained under 1:12.5 (biomass:DES ratio), 4.63 h (time) and 87 °C (temperature). Further, a dilute sulphuric acid (2%, *v*/*v*) hydrolysis was carried out to destabilize the hemicellulose that resulted in 23.7 ± 0.50 g/L of xylose. Fermentation of the obtained xylose was carried out using a red oleaginous yeast, *Rhodosporidium toruloides* NCIM 3547, with free and Ca^{2+}-alginate-immobilized cells for xylitol production under microaerophilic conditions and obtained yields of 4.73 ± 0.40 g/L (168 h) and 9.18 ± 0.10 g/L (packed bed reactor with a retention time of 18 h), respectively. Further, when the same fermentation was performed under aerobic conditions about 40.93 ± 0.73% lipid accumulation was observed with free cells. For saccharification, *Aspergillus-niger*-derived cellulase was used and this resulted in a yield of 27.45 ± 0.04 g/L of glucose. The glucose-enriched hydrolysate was supplemented for fermentation under nitrogen starved conditions from which 46.81 ± 2.60% (*w*/*w*) lipid content was obtained.

Keywords: water hyacinth; deep eutectic solvent; delignification; xylose; xylitol; lipids

Citation: Umai, R.D.; Jacob, S.; Kumar, V. Deep Eutectic Solvent Pretreatment of Water Hyacinth for Improved Holocellulosic Saccharification and Fermentative Co-Production of Xylitol and Lipids Using *Rhodosporidium toruloides* NCIM 3547. *Fermentation* **2022**, *8*, 591. https://doi.org/10.3390/fermentation8110591

Academic Editors: M. Ahsanul Islam and Williams Olughu

Received: 27 September 2022
Accepted: 27 October 2022
Published: 31 October 2022

1. Introduction

Water hyacinth (WH) (*Eichhornia crassipes*) is an invasive aquatic weed that spread rapidly on water bodies. It has been estimated that in a span of 8 months, these plants could propagate at a high rate that covers almost 0.4 ha of water surface, thus obstructing fishing and navigation [1]. It also decreases dissolved oxygen levels and prevents exposure and penetration of sunlight into water bodies, putting primary producer organisms such as phytoplankton at high risk. Even after the life cycle of the plant biomass, the natural decomposition of dead material that happens under the subsurface tends to reduce the pH to the acidic range, further lowering the dissolved oxygen with an emission of greenhouse gases such as CH_4, CO_2 and hydrogen sulphide [2]. These chemical changes to the aquatic ecosystem influence consequent fluctuations in the population of invertebrates and fish to depauperate communities [3]. Bai et al. [4] have made a consolidated framework for assessing the impact of invasive weeds with an index range of 1–4 based on social, economic and ecological implications. According to their report, it has been elucidated that WH scored 4 in terms of impact index and 3 for spread index, which reflects its negative impact on the ecosystem [5]. Consequently, WH should be eradicated from water bodies. At the same time, to strike the balance between the ecological and environmental sustainability, it is wiser to implement a valorization strategy or add value to the harvested

weed to get an economic advantage from the waste generation. WH contains significant cellulose (26.90%, *w/w*) and hemicellulose (24.50%, *w/w*), which prompts its usage as an effective feedstock for fermentative-driven value-added product synthesis. Several potential applications have been reported for WH such as phytoremediation, cellulose nanocrystals, composting, animal feed and even as a carbon source to produce biofuels, such as biodiesel, biogas and bioethanol [6,7].

A recent shift in the consumer preference for low glycemic index food products has triggered the market for alternative sweetener like xylitol. Xylitol's apparent effect on oral healthcare, especially as a sweetener in chewing gums, has created a rise in demand for xylitol in the market. It has been estimated that in 2020 the market occupancy of xylitol is about $0.901 billion and is expected to reach $1.10 billion by 2028, growing at a compounded annual growth of 2.59% from 2021 to 2028 [6]. Catalytic conversion of wood-based xylose to xylitol is the conventional strategy adopted to meet the market demand. Acid hydrolysis of biomass generates hemicellulosic hydrolysate consisting of xylose that is isolated and hydrogenated to produce xylitol. Resources such as birch bark, corn cob, pulp and paper waste are being used as a raw material for the xylose. However, the biotechnological method offers the possibilities of lowered cost and energy compared with the chemical methods [7]. D-Xylose metabolism by yeasts has been widely researched because of its high xylitol yield. Yeasts use xylose reductase (XR) and xylulose dehydrogenase (XDH) to reduce xylose to xylitol. The genus *Candida* (*C. guilliermondii*, *C. tropicalis* and *C.mogii*), has previously been shown to be capable of synthesizing xylitol from xylose generated from hydrolyzed agricultural biomass [8]. *Rhodosporidium toruloides*, an oleaginous yeast, has been reported to produce xylitol, arabitol from xylose and galactitol from galactose along with single cell oil (lipids) synthesis [7,8].

Though the WH contains significant holocellulose, the presence of lignin (5–8%, *w/w*) impedes the enzyme accessibility for saccharification, which prompts the adoption of a suitable pretreatment strategy. The increase in demand for cost effective and eco-benign pretreatment processes has led to the emergence of novel green solvents and ionic liquids (IL). Deep eutectic solvents (DESs) are a kind of an IL that has gained a recent prominence for pretreatment of lignocellulosic biomass (LCB) among the researchers as an alternate to harsh chemicals (acid/alkali) with the recovery of lignin by precipitation for its application to synthesize green chemicals [9]. DESs possess the benefits of IL, and moreover, they are affordable, biodegradable, simple to prepare, recyclable and produce less-toxic byproducts [10]. DESs in biorefinery are advantageous due to their versatility with pretreatment, extraction of lignin and catalysis capabilities in biomass/biowaste-to-biorefinery conversion processes, though its use in delignification is still in its nascent stage [11,12].

In this study, an attempt has been made to synthesize a DES using choline chloride (ChCl) (trimethyl ammonium chloride) and urea to delignify the WH biomass, which has not been reported elsewhere. Multivariate analysis of various independent parameters that significantly affect the DES treatment on different LCBs were investigated by Xu et al. [11] and Massayev and Lee [12]. It has been indicated that high treatment temperature with corresponding holding time and ratio of DES with biomass because of the viscous nature of the solvent were deemed to affect the lignocellulose treatment. Therefore, in this study, process parameters such as biomass (WH): DES ratio, treatment temperature (°C) and time (h) for maximum delignification were chosen for optimization using Box–Behnken Design (BBD)-based Response Surface Methodology (RSM). As hemicellulose and cellulose are the major polysaccharides that yield pentose (C5) and hexose (C6) sugars, respectively, a two-step saccharification was adopted as follows:

(i) A mild sulphuric acid (2%, *v/v*) for xylose (C5 sugar) recovery from hemicellulose;
(ii) Enzymes (a combination of cellulase and xylanase) derived from *Aspergillus niger* for hydrolysis of holocellulose to yield glucose and xylose as reported earlier by our research group [13].

To have complete utilization of these two forms of sugars (glucose and xylose) from WH hydrolysates, an effective fermentative process with *Rhodosporidium toruloides* NCIM

3547, an oleaginous red yeast that has been reported to produce xylitol from xylose and lipids from glucose, has been employed [14,15]. This yeast has been extensively used for LCB-derived sugar fermentation to lipids (40–70%, *w/w*) due to its tolerance for the effect of inhibitors present in the crude acid hydrolysate [16]. The accumulation of these by-products and their efflux has been postulated as an overflow metabolism under oxygen-limited conditions contributing to the redox balancing during xylose catabolism [17]. Therefore, it has been strategically planned to perform the fermentation of xylose derived from WH hydrolysate to xylitol under microaerophilic conditions and creating a nitrogen limitation for lipids synthesis from glucose. To the best of our knowledge, this is the first study to report a comprehensive treatment of WH with a DES and co-production of sugar alcohol (xylitol) and lipids using the *Rhodosporidium toruloides* NCIM 3547, as represented in Figure 1.

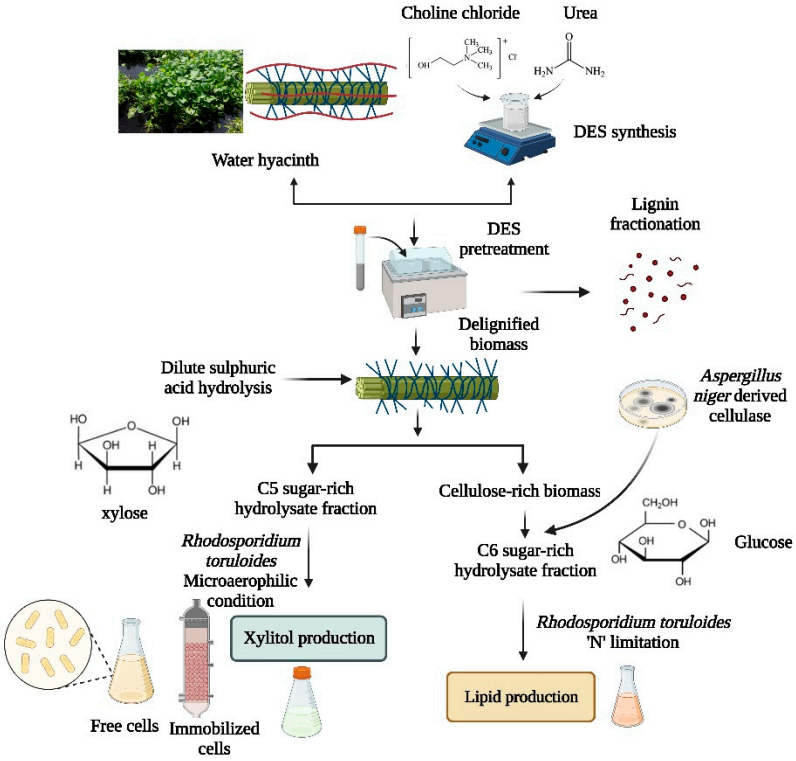

Figure 1. Flow of process adopted in the strategic utilization of cellulosic and hemicellulosic fractions of WH for xylitol and lipid synthesis using *Rhodosporidium toruloides* NCIM 3547.

Various parameters, including growth conditions, initial substrate concentration and the presence of inhibitors in the hydrolysates may affect xylitol synthesis by yeast [17]. Therefore, an alternative strategy of Ca^{2+} alginate immobilization and operating the xylitol fermentation in a packed bed reactor (PBR) has been attempted to test its effectiveness over the free-cell fermentation process, which has another advantage of reusing of the microbial inoculum for repeated cycles thereby increasing the fermentation efficiency.

2. Materials and Methods

2.1. Substrate: Water Hyacinth (WH)

Fresh WH was collected from a lake (Potheri: 12°49′03.6″ N 80°02′45.3″ E), Tamil Nadu, India. This lake serves as a natural habitat for migratory birds [18] and part of the lake has been infested with WH due to eutrophication (Supplementary material: Figure S1). Therefore, frequent eradication of WH from the lake to conserve the biodiversity is being routinely practised by the public authorities. For effective utilization of this discarded and unutilized WH biomass, a biovalorization route has been formulated through this study. The harvested WH was washed several times with tap water to remove adhering dirt and

then cut into pieces, solar dried to remove excessive water content and then oven dried and powdered. The biomass powder was sieved through a mesh to a particle size of 22 µm and this was used for further studies. The biomass was characterized for proximate and biochemical parameters and the results are tabulated in Table 1.

Table 1. Characterization of substrate, DES and enzymes employed in this study.

Components	Parameters	Value
Substrate - WH	Moisture content (%, *w/w*) [a]	94.20 ± 0.75
	Total solids (%, *w/w*) [a]	5.80 ± 0.75
	Ash content (%, *w/w*) [b]	21.50 ± 0.20
	Volatile solids (%, *w/w*) [b]	78.44 ± 0.20
	Cellulose (%, *w/w*) [b]	26.90 ± 1.76
	Hemicellulose (%, *w/w*) [b]	24.50 ±1.71
	Lignin (%, *w/w*) [b]	5.68 ± 0.24
DES (Choline chloride: urea)	Density (g/mL)	1.116 ± 0.02
	Solubility	Miscible Acetic acid, Ethanol, Water Immiscible Toluene, Chloroform
Enzyme activity(*Aspergillus niger*)	Carboxy methyl cellulase (CMC-ase) (IU/mL)	6.23
	Filter paper units (FPU/mL)	0.77
	Xylanase (IU/mL)	2.21

[a] wet weight basis; [b] dry weight basis. The values represent mean ± standard deviation.

2.2. Microorganism and Inoculum Preparation

Rhodosporidium toruloides NCIM 3547, a red yeast of oleaginous nature was obtained from the National Collection of Industrial Microorganisms (NCIM), Pune, India. YEPD agar media (Yeast extract—10 (g/L); peptone—10 (g/L); dextrose—20 (g/L); and agar—20 (g/L)) was used for routine subculturing and maintenance of the mother culture. Further, to make the strain adaptable to the desired carbon source an enrichment media that contained: xylose—5% (*w*/*v*); yeast extract—3 g/L; $MgSO_4$—2 g/L; NaCl—2 g/L; KH_2PO_4—1.5 g/L, was used.

2.3. Adaptive Laboratory Evolution (ALE) Strategy for Rhodosporidium toruloides NCIM 3547 to Produce Xylitol

ALE strategy aids in the adaptation of fermentative microbes to the actual complex hydrolysate sugars that might be mixed with other intermediates [19]. ALE was carried out with successive subculturing of the inoculum at an interval of 96 h for a period of 30 days in broth that contained 15% (*v*/*v*); 25% (*v*/*v*) and 40% (*v*/*v*) of WH hydrolysate with 20 ± 5 (g/L) of xylose and 5 ± 1.5 g/L of glucose obtained from 2% (*v*/*v*) H_2SO_4 acid treatment. The adaptation phase included the induction of microaerophilic conditions by supplementation of sodium thioglycollate 1 mL/L into the growth medium that induced xylitol synthesis. The xylitol production by *Rhodosporidium toruloides* NCIM 3547 under the ALE was confirmed by the HPLC analysis of the fermented broth (Supplementary material: Figure S2) based on the retention time of a xylitol standard (Sigma Aldrich, 99.9% pure). The logarithmic phase culture broth at 40% (*v*/*v*) WH hydrolysate supplementation that had an O.D = 1.5 (36 h) was used as an inoculum for xylitol fermentation experiments.

2.4. Synthesis of DES and Pretreatment

The DES was prepared with choline chloride (ChCl) as Hydrogen Bond Acceptor (HBA) and urea as Hydrogen Bond Donor (HBD). The DES components were taken at a molar ratio of 1:2 and heated at 60 °C until a homogeneous colourless liquid was formed [20]. Solvent characteristics such as density and miscibility with different solvents were de-

termined based on standard methods [20]. The characteristics of the synthesized DES have been tabulated in Table 1. Further, Fourier Transform Infrared (FTIR) spectrometer (Agilent Technologies, Cary 600 Series, Santa Clara, CA, USA) was used to confirm the formation of the DES based on the functional groups present in the pure compounds (ChCl and urea) and the synthesized DES in the range of 400 to 4000 cm^{-1}.

2.5. Pretreatment of WH by DES and Recovery of Lignin

Selection of a range of variables from the chosen parameters for DES pretreatment was performed via the OVAT (one variable at a time) approach. Different ratios of WH:DES (ranging from 1:5 to 1:25, g/g), reaction periods (2 to 6 h) and temperatures (70 to 95 °C) were selected and pretreatment was carried out. DES pretreatment was performed below 95 °C in contradiction to reported recommended high temperature conditions (>100 °C) to minimize energy input, which is beneficial for industrial processes [21]. In addition, Procentese et al. [22] reported that high solid recovery was possible with ChCl:urea when the temperature is maintained at 80 °C. The pretreated biomass was recovered by filtration and dried. Lignin content of raw WH and DES-pretreated WH was estimated by the titration method [23].

Delignification percentage was calculated using the Equation (1).

$$\text{Delignification\% } (w/w) = \frac{(\text{Lignin\% in raw WH} - \text{Lignin\% in treated WH})}{\text{Lignin\% in raw WH}} \times 100 \quad (1)$$

2.6. Statistical Optimization of DES Pretreatment by BBD-RSM

BBD followed by RSM was used to predict the influence of independent experimental factors and their interaction for maximum delignification with different input values of the factors. A three-level-three-factor BBD was employed to generate 17 experiments by considering the process parameters (factors) with boundary conditions obtained after OVAT (Supplementary material: Figure S3a–c) as follows: biomass:DES ratio of 1:10 to 1:20; time of 3 h to 5 h; and temperature of 80 °C to 90 °C. All the run order experiments were carried out in triplicate. The experimental data obtained through BBD was used to generate the best-fit second-order polynomial quadratic regression equation as given in Equation (2).

$$Y = \beta_0 + \beta_1 A + \beta_2 B + \beta_3 C + \beta_{11} A2 + \beta_{22} B2 + \beta_{33} C2 + \beta_{12} AB + \beta_{23} BC + \beta_{13} AC \quad (2)$$

where, Y is the dependent variable (delignification % of WH), β_0, β_1, β_2 and β_3 are the coefficients of linear terms, β_{11}, β_{22} and β_{33} are quadratic coefficients and β_{12}, β_{23} and β_{13} were interaction coefficients. A, B and C represent the selected independent variables/factors biomass:DES ratio, treatment time (h) and temperature (°C), respectively. The effect of the parameters and their interaction on the response has been studied by conducting significance tests and analysis of variance (ANOVA) on each response to check the adequacy of the model. The optimized variables for the process have been chosen through the response optimizer function of MINITAB 14 software. Validation experiments were conducted in triplicates based on the optimal process parameters and the observed delignification was compared with the predicted delignification to estimate the standard error %.

2.7. Recovery of Delignified WH and Lignin after DES Pretreatment

Recovery of lignin from the DES pretreatment process under optimized conditions was performed as reported in the literature [24]. The WH:DES reaction was stopped with the addition of 100 mL of ethanol as an anti-solvent, after which the warm mixture was filtered through a sintered filter attached with a vacuum filtration unit and the solid residue was washed with warm water followed by drying at 60 °C until constant weight attainment that represented the delignified WH biomass. As lignin recovery is an important step in DES pretreatment, to the ethanol–DES filtrate about twice the volume of water (~200 mL) was added and the solution was acidified with 1 N HCl. This suspension was allowed to stand overnight for the lignin to become precipitated. After checking the precipitated

lignin, either the suspension can be vacuum filtered or centrifuged at 10,000 rpm for 15 min. The obtained lignin solid was washed with a water–ethanol (9:1) mixture to remove traces of DES and dried in an oven at 60 °C until a constant weight was obtained.

2.8. Characterization of Raw and Treated WH

The morphology of the raw and DES-pretreated WH was analysed using scanning electron microscopy (SEM) at 30 kV (SNE- 3200M, SEC- DESKTOP Mini-SEM). X-ray diffraction (XRD) spectrometry (Malvern Panalytical, AERIS-High-resolution benchtop XRD, Malvern, UK) was employed to ensure the amorphous lignin removal and exposure of crystalline cellulose. The crystallinity index (*CrI*) was determined to calculate the percentage of crystalline material in the biomass as given in Equation (3) [25].

$$CrI\% = (I_{002} - I_{am})/I_{002} \times 100 \quad (3)$$

where, I_{002} = maximum intensity at 22°, I_{am} = minimum intensity at 18°.

The raw and DES-pretreated WH were analysed using FTIR within the wavelength range of 4000–400 cm^{-1} using FTIR spectrometer (Agilent Technologies, Cary 600 Series, USA) to understand the chemical transformation after DES pretreatment.

2.9. Hemicellulosic Hydrolysate Preparation

Dilute acid hydrolysis of DES-pretreated WH was performed using 2% (*v*/*v*) of sulphuric acid at a solid-to-liquid ratio of 1:10 (*w*/*v*) for 20 min at 121 °C to obtain a hemicellulosic hydrolysate as reported by Narisetty et al. [26]. The glucose and xylose present in the hydrolysates were estimated using standard biochemical assays, viz., the dinitrosalicylic acid (DNS) method [27] and the orcinol method that involves Bial's reagent [28], respectively. The Bial's reagent was prepared by dissolving 0.3 g orcinol and 0.05 g ferric chloride in 100 mL concentrated hydrochloric acid. To 0.5 mL hydrolysate, 1 mL of reagent was added and incubated in a boiling water bath for 5 min. The xylose standard graph was plotted with 100–500 µg of xylose. The colour intensity that developed was read at 617 nm in a spectrophotometer. The concentration of xylose was calculated using the linear equation of the standard plot with a regression coefficient (R^2) of 0.9829 (Supplementary material Figure S4a).

2.10. Enzymatic Cellulose Hydrolysis of DES Delignified WH

Crude enzymes (cellulase and xylanase) derived from *Aspergillus niger* were employed for cellulose hydrolysis of DES-pretreated WH biomass using a solid-to-liquid ratio 1:18 (*w*/*v*) at 50 °C for 6 h. In this study, DES-pretreated WH biomass was mixed with the crude enzymes at a ratio of 1:18 (*w*/*v*); the obtained optimal cellulase and xylanase activity is given in Table 1. After incubation, the biomass was separated from the reaction solution by centrifugation at 8000 rpm for 15 min. The resulting supernatant (hydrolysate) was analysed for reducing sugars (glucose and xylose).

2.11. Fermentation of Hemicellulosic and Cellulosic Hydrolysate for Co-Production of Xylitol and Lipids

As the candidate yeast *Rhodosporidium toruloides* is capable of utilizing the xylose and glucose by exhibiting a diauxic growth pattern [29], the fermentation was performed in three ways, as represented in Figure 1, for co-production of xylitol and lipids. The xylose fermentation media for xylitol and Yeast Basal Media (YBM) for lipid synthesis were adapted from Narisetty et al. [26] and Alankar et al. [30], respectively. Xylitol production in *Rhodosporidium* (*Rhodotorula* sp.,) is reported to be oxidative stress induced [15]. Therefore, in this study, under shake-flask (100 mL) fermentation, microaerophilic conditions were deployed by adding 1 mL/L of sodium thioglycolate (10%, *w*/*v*) in 25 mL of the WH acid hydrolysate along with the following minimal media components (g/L): $CuSO_4.5H_2O$—0.001, KH_2PO_4—2, $MnSO_4.H_2O$—0.003, $MgSO_4.7H_2O$—0.4, and yeast extract—1.5. The fermentation was carried out for a period of 168 h until there was a stability in the biomass yield and the

xylose consumption pattern. Intermittent analysis of the sugars (xylose and glucose), xylitol and biomass growth were performed. For lipid synthesis, 'nitrogen (N)' limitation conditions were induced by reducing the yeast extract from 3 g/L to 0.5 g/L and adding ammonium sulphate (1 g/L) as an inorganic 'N' source while retaining the rest of the composition.

2.12. PBR Studies with Immobilized Rhodosporidium toruloides for Xylitol Production

Immobilization of *R. toruloides* was carried out via the cell entrapment method using sodium alginate (2% *w*/*v*) and calcium chloride (0.3 M) with 10% (*v*/*v*) of yeast. In this study, in order to check the efficiency of the immobilized cells for further reuse, the fermentation process was carried out in two cycles with fresh hydrolysates deployed for each cycle in a PBR. The Ca^{2+}-alginate-immobilized beads were packed in the PBR for fermentation of WH sugar hydrolysates. The WH hydrolysate with 23.7 ± 0.50 g/L of xylose as the major 'carbon (C)' source was used as a feed for the PBR. After the first cycle of fermentation for 18 h (no drastic change in xylose depletion), fresh hydrolysate was fed to the PBR to check the adequacy of the immobilized cells for repeated production cycles.

2.13. Product Analytical Methods

2.13.1. Xylitol Analysis: Colorimetric Method and HPLC

The xylitol produced during the fermentation was estimated by the colorimetric method adapted from Sánchez [31] and involving periodate oxidation followed by the Hantzsch reaction. The fermented broth was incubated at room temperature for 60 s with reagent 1 (0.5 mL of 0.5 M formate (pH 3.0) and 0.3 mL of 5 mM sodium periodate). To this solution, 0.3 mL of reagent 2 (0.1 M acetylacetone, 2 M ammonium acetate and 0.02 M sodium thiosulphate) was added and incubated in the boiling water bath for 2 min. The solution was cooled and the colour intensity measured at 412 nm. The same procedure was adapted to plot the standard graph using a 50–200 µg/mL concentration of xylitol. The concentration of xylitol in the fermented broth was calculated using the linear equation of the standard plot with a regression coefficient (R^2) of 0.9942 (Supplementary material Figure S4b).

Further confirmation of xylitol in the broth was conducted using High Performance Liquid Chromatography (HPLC). The samples were filtered through a 0.22 µm nylon syringe filter (RanDisc syringe filter). The analysis was carried out with the Shimadzu LC-20AD HPLC system and an NH_2-reverse phase (RP) column (4.6 mm × 250 mm × 5 µm) with a refractive index detector (RID). The mobile phase consisted of acetonitrile:water (80:20) with a flow rate of 0.8 mL/min at ambient temperature. An injection volume of 20 µL was maintained for both standard and hydrolysate samples.

2.13.2. Lipid and Fatty Acid Methyl Ester (FAME) Analysis by GC-MS

Extraction of lipids from *R. toruloides* was carried out by the method described by Bligh and Dyer [32]. Lipid content as a percentage of biomass dry weight was calculated using the formula given in Equation (4).

$$\text{Lipd content } (\%) = \frac{\text{Lipid weight (g)}}{\text{dry cell weight(g)}} \times 100 \quad (4)$$

The resulting lipids from the oleaginous yeast obtained through the fermentation were treated with a 2:1 ratio of n-hexane and methanolic KOH (2 M) and incubated for 20 min at 70 °C. After incubation, about 1.2 mL of 1 M HCl was added with gentle stirring followed by addition of n-hexane (1 mL) for the phase separation. The upper aqueous layer containing the fatty acid methyl ester (FAME) was subjected to gas chromatography–mass spectrometry (GC-MS) (GCMS-Shimadzu QP2010 system, Japan) with an Sh-Rtx-5 column (30 m × 0.25 mm × 0.25 µm). The column temperature was maintained at 50 °C to 300 °C at a rate of 7.5 °C/min and a hold-time of 2 min. Helium as a carrier gas was provided and maintained at a constant flow rate of about 3.0 mL/min with a 1:10 split ratio. The data

obtained were evaluated using the NIST/EPA/NIH Mass Spectral Library (NIST 14) and the NIST Mass Spectral Search Program (Version 2.2).

2.13.3. Kinetic Studies on Different Fermentative Strategies

In this study, an attempt has been made to analyse the dynamics in the kinetic behaviour of the fermentation when xylose and glucose enriched WH hydrolysates were supplemented and its effect towards the biomass yield, growth rate, xylitol production and lipid accumulation using *R. toruloides* NCIM 3547 through the Luedeking–Piret model equation [33], as represented in Equation (5).

$$Xt = \frac{X_o \times X_{max} e^{\mu_{max} t}}{X_{max} - X_o + X_o e^{\mu_{max} t}} \quad (5)$$

where, X (g/L) is the biomass concentration at any time t (h); μ_{max} (h^{-1}) is the maximum specific growth rate; X_{max} (g/L) is the maximum biomass concentration in the fermentation medium; Xt and X_0 are biomass during fermentation period of 't'h and initial ('0')h', respectively. A non-linear regression solver method using MS Excel was used to solve the kinetic model equation and obtain parameters such as X_{max} and μ_{max}.

The following equations were used to calculate substrate uptake efficiency (Equation (6)), xylitol productivity (Equation (7)) and xylitol and lipid yield coefficient (Equations (8) and (9), respectively).

$$\text{Efficiency of utilization of substrate } (\%) = \frac{[S]_i - [S]_f}{[S]_i} \times 100 \quad (6)$$

where, reducing sugar substrate—glucose and xylose; $[S]_i$ = initial sugar concentration (g/L); $[S]_f$ = final sugar concentration (g/L).

$$\text{Xylitol productivity } \left(\frac{g}{L\ .h}\right) = \frac{\text{Maximum concentration of xylitol } (g/L)}{\text{Fermentation time } (h)} \quad (7)$$

Further, xylitol and lipid yield coefficients were calculated based on Equations (8) and (9).

$$\text{Xylitol yield coefficient } [Y_{\frac{p(X)}{s}}] = \frac{\Delta P}{\Delta S} = \frac{P - P_0}{S - S_0} (g/g) \quad (8)$$

$$\text{Lipid yield coefficient } [Y_{\frac{p(L)}{s}}] = \frac{\Delta P}{\Delta S} = \frac{P - P_0}{S - S_0} (g/g) \quad (9)$$

where, ΔP = change in xylitol/lipid concentration (g/L); ΔS = change in substrate concentration (g/L).

3. Results

3.1. Proximate and Biochemical Analysis of the WH

WH being considered as an LCB differs from other terrestrial biomass due to its excessive moisture content (94.20%, Table 1) and might need drying before its storage until further processing. Solar drying of wet biomass was performed that could alleviate 80% of the moisture, which was further removed to obtain the dry biomass (5.80%, *w/w*, wet weight basis). From the proximate analysis, it has been observed that WH contained 78.44% (*w/w*, dry weight basis) of volatile solids that exemplify the rich organic matter capable of valorization through the biological route that corroborated with the characteristics study on WH by Alankar et al. [30]. However, these parameters depend on the maturing stage of the plant and its geographical location and thereby differ slightly from other reported literature regarding WH [34,35]. From the biochemical analysis, it has been observed that cellulose (26.90%, *w/w*) and hemicellulose (24.50%, *w/w*) are almost in equal proportion and that paves the way for valorizing both pentose and hexose sugars through fermentation. As WH has been explored mostly on their cellulosic sugar components for diversified

products [36–38], tapping its hemicellulose potential along with its cellulosic fraction for multi-product development seems to be promising in complete utilization of this biomass.

The biochemical composition of WH aligns with the reported range by Wauton et al. [39]. The holocellulosic (cellulose and hemicellulose) portion of WH is bound by recalcitrant lignin (5.68%, *w/w*), which necessitates an efficient pretreatment strategy. To address this issue of lignin and to enable digestion of the carbohydrate polymers easily, a suitable pretreatment procedure is necessary [40,41]. Though a variety of delignification options are available, a good pretreatment strategy should not only increase the digestibility of lignin components but also facilitate the recovery of holocellulose and lignin [40]. Hence, the DES method was adopted by considering the aforementioned factors for biomass pretreatment.

3.2. Properties of Synthesized DES Using ChCl:Urea

The ChCl:urea-based DES synthesized in this study was subjected for analysis to ensure the nature of it towards the WH pretreatment. From the results (Table 1), it has been observed that the density of the DES formed was 1.116 g/mL at 30 °C, which is in agreement with the result reported by Zhang et al. [42,43]. The fact that DESs contain both cationic and anionic species, as well as non-ionic species, has facilitated their capacity to dissolve in a wide variety of solvents. It was observed that the ChCl:urea DES was miscible in water, acetic acid and ethanol and immiscible in toluene and chloroform. The results show that the synthesized DES might be categorized as a hydrophilic DES as reported by Shafie et al. [44]. Further, the formation of the DES and the interaction between the two compounds (ChCl and urea) was inferred based on the FTIR spectra (Supplementary material: Figure S5a–c). The band spectra around the 3300 cm^{-1} regions were observed to be broader in the DES compared to that in the ChCl and urea, which indicated the formation of hydrogen bonds between the HBA and HBD [45,46]. The band in choline chloride around the 1080 cm^{-1} and 950 cm^{-1} regions, that also appeared in the synthesized DES, shows that the -CH structure has not been altered [47]. Wang et al. [46] studied the effect of an acetate (CH_3COO^-)-based IL and ChCl:urea-based DES for solubilization of xylan through molecular dynamic simulation. It was concluded that ChCl:urea in a 1:2 ratio had an efficient interaction of highly condensed molecular networks in xylan and lignin because of their effective HBA and HBD combination.

3.3. Effect of Process Parameters Ascertained by OVAT Analysis

For delignification of WH three significant process parameters, biomass:DES ratio, process time and temperature were selected. From the obtained results, it can be seen that delignification increased when the WH:DES ratio increased from 1:5 to 1:10 and 1:15 (g/g). This increase can be explained by the fact that the increase in the WH:DES ratio resulted in more DES available to react with WH. The delignification is due to the hydrogen bond formation between the donor and acceptor, which led to the formation of the DES, that caused the cleavage of the β-O-4 bonds between lignin monomers and between the lignin–hemicellulose complex. Further, a hydrogen bond is formed between lignin monomers and chloride anions, which enhances the solubility of the lignin in the DES [46,47]. However, in WH:DES ratios of 1:20 and 1:25 there was a decrease in the delignification percentage. This might be due to the reason that a high concentration of DES might cause a highly viscous nature and limit the interaction of DES on biomass, as reported in the literature [48,49]. There was an increase in the delignification percentage with an increase in time (up to 4 h) and temperature (up to 90 °C). The increase in time and temperature enhanced the dissociation of the components of WH, which might lead to the solubilization of lignin in the DES. At a longer time (6 h) and a higher temperature (95 °C), there was a decrease in delignification that might possibly be due to the condensation of lignin that resulted in a decrease in its solubility in the DES as reported by Wang et al. [50]. Based on the range chosen from the OVAT for the selected parameters, further optimization was performed using the BBD-RSM.

3.4. Optimization of DES Pretreatment by BBD-Based RSM

BBD was employed in the process optimization to generate higher-order response surfaces with fewer required runs for determining the global optima than the factorial-based methods. In this study, process optimization was performed with the boundary conditions as follows: biomass:DES ratio (A) (1:10 to 1:20), temperature (B) (80 to 90 °C) and time (C) (3 to 5 h). Based on the design, 17 experiments were carried out and delignification percentages were determined as tabulated in Table 2. The statistical significance of the chosen variables towards the delignification was analysed based on the ANOVA, as indicated in Table 3. From the Table 3, it can be observed that the model F-value of 273.61 implies the model is significant. *p*-Values <0.05 indicate model terms (factors) are significant towards the delignification. In this study, A, B, C, BC, B^2, C^2, A^2C and AB^2 are found to be significant, demonstrating the individual and interactive effect of the variables on WH delignification. Values greater than 0.1 indicate the model terms are not significant. The lack-of-fit F-value of 2.49 implies that the lack of fit is not significant relative to the pure error. A non-significant lack of fit is good and therefore the model is deemed to be fit. The regression coefficient (R^2), which denotes the fitness of the model, was 0.9983 after the removal of insignificant interactions such as AC, A^2 and C^2 based on the ANOVA (Table 3) and the adjusted R^2 was 0.9947 (Figure 2d), thereby justifying the suitability of BBD-based RSM for finding the global optima for DES-based WH delignification. The residual plots obtained for the regression model have been presented in Supplementary Figure S6. The quadratic equation (Equation (10)) for regression was obtained as follows:

$$\begin{aligned} \text{WH Delignification } (\%) = 50.30 + 2.52 \times \text{ A} + 3.57 \times \text{ B} - 6.20 \times \\ \text{C} - 0.6225 \times \text{ AB} + 2.80 \times \text{ BC} + 9.11 \times \text{B}^2 + 5.51 \times \text{A}^2\text{C} - 8.12 \times \text{AB}^2 \end{aligned} \quad (10)$$

where, A represents the biomass:DES ratio, B represents the temperature and C represents the time of DES pretreatment. The optimized process parameters predicted through point prediction were: biomass:DES—1:12.5; time—4.63 h; and temperature—87 °C, and resulted in a maximum delignification of 64.32 ± 4.08% (*w/w*), which is close to the predicted value of 68.96% (*w/w*). The 3D surface plots representing the interaction of the parameters are shown in Figure 2a–c that depict the correlation of biomass:DES, time and temperature to be an influencing factor towards delignification. It has been proven that the solvation and dissolution of biomass by DES is strongly dependent on the operating temperature and time [51]. From the response surface plot (Figure 2c) and Table 3, it has been observed that the temperature and time had a positive interactive effect towards the dependent parameter, i.e., delignification. When there is an increase in temperature with concomitant time, there was found to be an increase in the delignification % from 48% to 69%. Upon reaction of DES with any LCB there might be a possibility of different reactions such as hydrogenolysis, dehydration, hydrogenation, decarboxylation, aromatization or isomerization that prompts random cleavage of C–C and C–O bonds in the representative units of biomass that could yield different degradation products [51]. Procentese et al. [22] demonstrated the efficiency of three different DES with ChCl as the HBA and glycerol, urea and imidazole as an HBD upon corn cob pretreatment with various temperatures from 80 to 150 °C by keeping a constant 1:15 solid-to-liquid ratio. The results indicated that only ChCl:urea was found to be effective at the reduced temperature of 80 °C and high solid recovery was possible only when the temperature was maintained below 120 °C for DES-based pretreatment; above this temperature there is a change in the viscous nature of the biomass:DES mixture that impedes the solid recovery after the pretreatment (Figure 2c). From the BBD-RSM optimization strategy, it has been observed that 64.32% of delignification was obtained with a recovery of almost 57.32% of lignin as a solid form from the original lignin fraction. Therefore, this DES pretreatment could be effectively adopted for favourable recovery of lignin and reusing the DES for multiple cycles, thereby affording the cost–benefit advantage and techno-economic feasibility.

Table 2. BBD-based run of experiments for DES pretreatment and the observed delignification.

Run Order	Biomass:DES Ratio	Temperature (°C)	Time (h)	Delignification% *
1	15	90	5	58.57 ± 2.63
2	10	85	5	45.92 ± 2.06
3	10	80	4	60.33 ± 2.77
4	15	80	3	64.33 ± 3.85
5	10	90	4	69.22 ± 3.11
6	20	85	3	52.33 ± 2.35
7	15	85	4	50.25 ± 2.26
8	15	90	3	65.37 ± 1.94
9	15	85	4	50.36 ± 2.11
10	10	85	3	47.67 ± 1.90
11	20	85	5	51.33 ± 2.56
12	20	80	4	50.37 ± 1.91
13	15	80	5	46.33 ± 1.38
14	15	85	4	49.62 ± 2.48
15	15	85	4	50.88 ± 3.05
16	20	90	4	56.77 ± 2.27
17	15	85	4	50.37 ± 2.01

* All experiments were done in triplicates and the values represent mean ± standard deviation.

Table 3. ANOVA for the BBD-RSM optimization of DES pretreatment.

Source	Sum of Squares	Degree of freedom	Mean Square	F-Value	*p*-Value	
Model	791.39	11	71.94	273.61	<0.0001	significant
A—Biomass:DES	25.35	1	25.35	96.41	0.0002	
B—Temperature	102.03	1	102.03	388.03	<0.0001	
C—Time	153.76	1	153.76	584.76	<0.0001	
AB	1.55	1	1.55	5.89	0.05	
BC	31.36	1	31.36	119.26	0.0001	
A^2	0.2237	1	0.2237	0.8508	0.3987	
B^2	349.21	1	349.21	1328.07	<0.0001	
A^2C	60.78	1	60.78	231.13	<0.0001	
AB^2	131.87	1	131.87	501.50	<0.0001	
Residual	1.31	5	0.2629			
Lack of Fit	0.5050	1	0.5050	2.49	0.1894	not significant
Pure Error	0.8097	4	0.2024			
Cor Total	792.71	16				

Lee et al. [52] suggested that DESs (ChCl:lactic acid and ChCl:urea) assisted with ultrasonication has improved digestibility of lignin and cellulose that is present in oil palm empty fruit bunches with enhanced sugar recovery. Possibly, the upgradation WH-DES pretreatment could be attempted as an extension of this study by having hybrid pretreatment strategies rather than as sole pretreating agent.

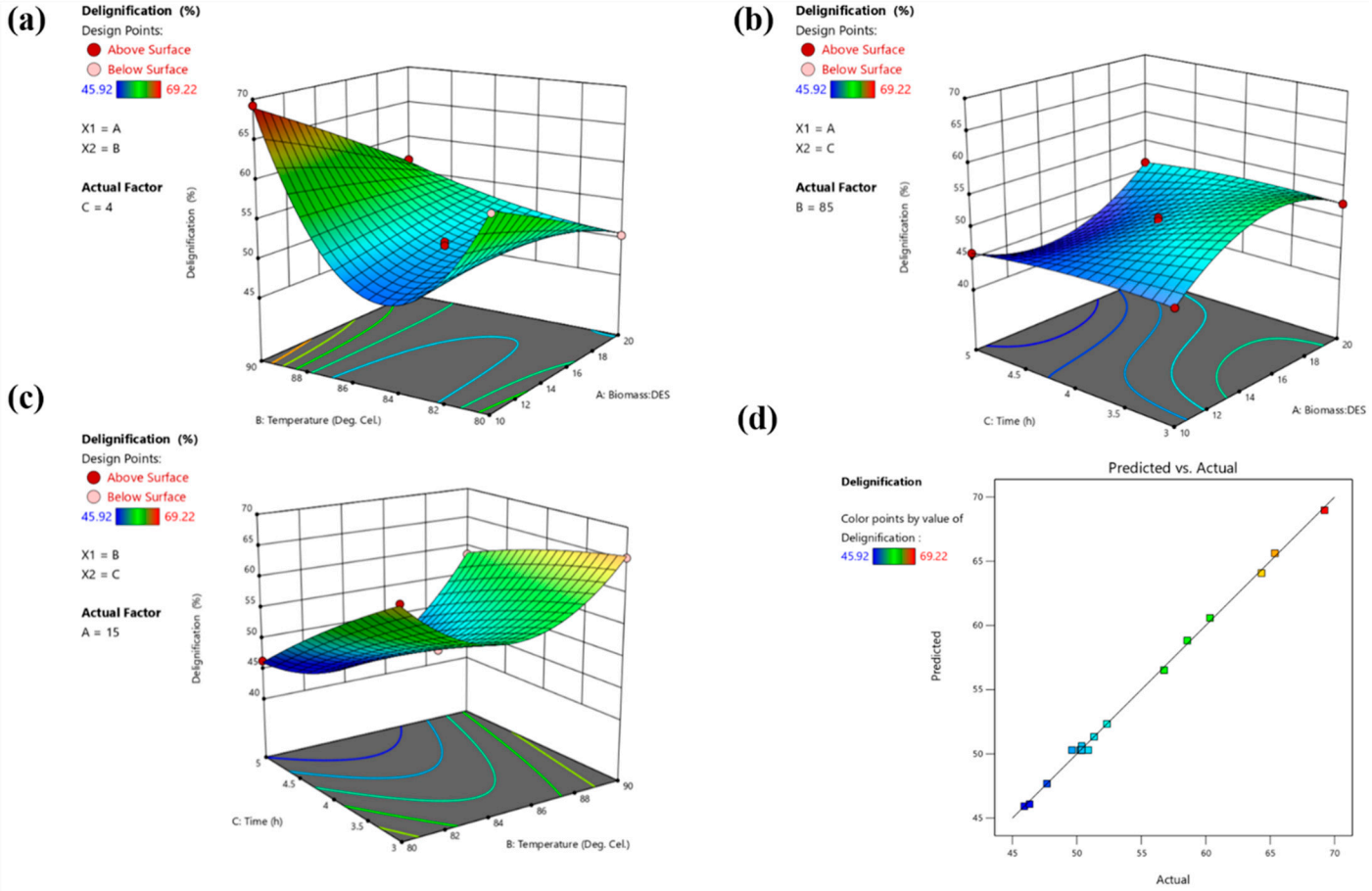

Figure 2. Three-dimensional surface plots representing the interactive effects of (**a**) biomass:DES vs. temperature; (**b**) biomass:DES vs. time; and (**c**) time vs. temperature on WH delignification. (**d**) Interactive plot of observed and theoretical WH delignification from BBD-RSM-based optimization.

3.5. Effect of DES Pretreatment on WH Based on SEM, FTIR and XRD

The morphological changes between the raw and DES-treated WH samples were studied using SEM. The raw WH showed a smooth and regular surface, as shown in Figure 3a, whereas the surface of the pretreated WH was damaged and irregular, which indicates lignin disruption (Figure 3b). Based on the FTIR profile of DES-pretreated WH (Figure 3c,d), it has been observed that the hydroxyl stretches at around 3300 cm^{-1} and deep peaks are observed for cellulose [53]. The fact that the intensity of the peak decreased following DES pretreatment demonstrates that the hydrogen bonds in cellulose has been disrupted to some degree due to lignin removal [54]. The peak at 2358 cm^{-1} indicates the acetal groups of cellulose. Appearance of this peak after DES pretreatment shows that cellulose has been exposed as a result of the removal of lignin [55]. The peak at 1614 cm^{-1} corresponds to the C=C stretching of aromatic groups associated with lignin. After DES pretreatment, it has been observed that there is a reduction in the intensity of this peak, denoting that lignin is removed [56]. Similarly, the intensity of the peak around 1419 cm^{-1} to 1421 cm^{-1} and 1247 cm^{-1}, which corresponds to aromatic group vibrations of lignin, has decreased after DES pretreatment [57]. The peak at 1369 cm^{-1} indicates the O-H group of phenol without ether linkage, which suggests that the β-O-4 ether linkage in lignin has been disrupted [58]. From the FTIR analysis, it can be understood that DES pretreatment efficiently breaks the bond between lignin and hemicellulose, allowing the biomass components to be separated.

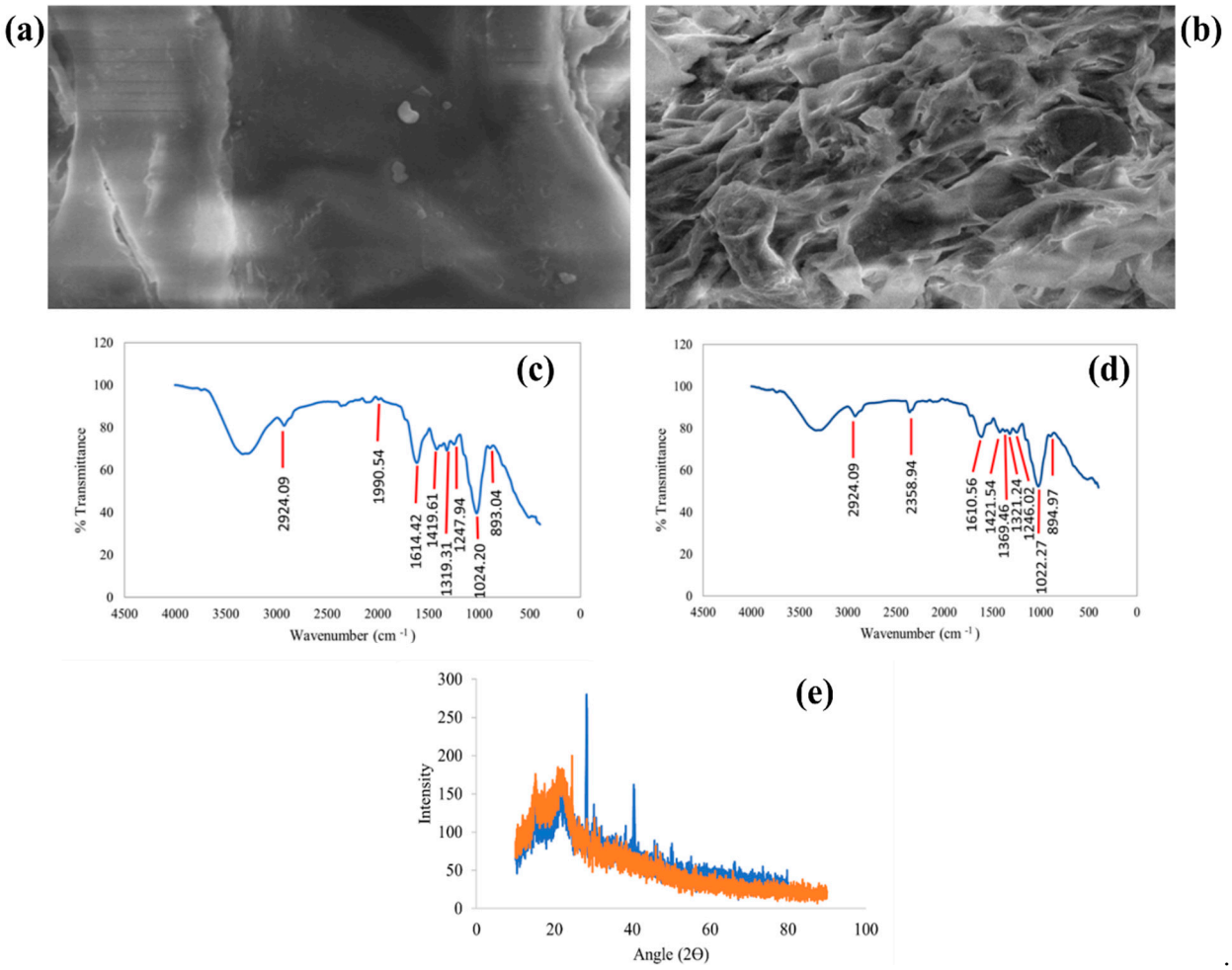

Figure 3. SEM image of (**a**) raw WH and (**b**) DES-pretreated WH. (**c**) FTIR spectra of raw WH and (**d**) FTIR spectra of DES-pretreated WH. (**e**) XRD spectra of raw WH (blue) with WH after DES pretreatment (orange) (pretreatment conditions include biomass:DES—1:12.5; time—4.63 h and temperature—87 °C).

SEM and XRD studies were performed both before and after the DES pretreatment in order to have a better understanding of the structural and morphological influence that DES pretreatment had on WH. From the SEM analysis, the surface of the WH was even and smooth before pretreatment, but the surface of the pretreated WH was damaged and uneven, which shows that the outer lignin layer has been disrupted. The extent of surface destruction was more in the DES-treated WH, suggesting that depolymerization of lignin has occurred, which can be correlated with the results of delignification [58]. Chen and Mu [59] reported that DES has induced a loosening and swelling effect on the cellulose fibre structure which could aid in enhanced saccharification due to the enzyme accessibility for binding. XRD data showed a slight increase in the CrI after DES pretreatment (Figure 3e). Cellulose is basically crystalline, therefore the increase in CrI is likely due to delignification and solubilization of hemicellulose (amorphous) [13,60]. Because of the recent increase in utilizing the lignin derived from LCB for synthesis of platform chemicals and nano-formulations, there is a requirement to reorient the pretreatment strategy adopted for delignification since conventional pretreatment strategies such as steam explosion, ultrasound, microwave, acid, alkali and ammonia that are widely employed for removal of lignin which do not include the recovery of it for further application. However, recent mild chemical treatments such as IL, organosolv and DES could favour the lignin macromolecule fractionation that is employed in nano-materials, furanic derivatives, bio-alkanes and other

green chemicals, which is deemed to be a suitable sustainable alternative approach for refining the biomass components [61]. Hence, for WH delignification, DES was employed for the fractionation of lignin.

The change in the functional groups between the raw and DES-treated WH were identified by FTIR, as shown in Figure 3c,d. A decrease in the peaks corresponding to lignin functional groups and the appearance of peaks pertaining to cellulosic functional groups were observed, which denotes the removal of lignin and exposure of cellulose and hemicellulosic fragments by the ChCl:urea DES. From the XRD analysis (Figure 3e), the CrI of raw and treated WH can be elucidated. In this study, the CrI of raw WH was found to be 40.13% and it was increased to 41.20% in the DES-treated WH. In contrast to this, Procentese et al. [22] reported that the CrI was reduced after ChCl:urea treatment at 80 °C in corn cob. The structural composition of this sample is statistically identical with the raw biomass, which is same as the outcome of this study. The marginal increase in the crystallinity in the DES-treated sample is therefore likely due to the amorphous lignin removal and exposure of cellulose, which is crystalline as indicated by the characteristic cellulose I peak in the treated biomass; this could enhance the enzymatic action of cellulase with improved digestibility as suggested by Fu and Mazza [61]. As the DES involves only the dissociation reaction with lignin under alkaline conditions, inhibitors such as acetic acid, furfurals and 5-HMF was less profound and these inhibitors are found to be at sub-inhibitory levels for yeast strains, as explained by Wood et al. [62].

3.6. Stepwise Saccharification of DES-Pretreated WH

The DES-pretreated WH was subjected to a stepwise saccharification process to obtain the hemicellulosic- and cellulosic-derived C5 and C6 sugars, respectively. On the other hand, the effect of DES pretreatment towards the yield of sugars from the WH biomass was compared between the raw and delignified biomass. In the first stage, mild acid treatment, the hydrolysate obtained from the dilute acid hydrolysis of DES-pretreated biomass yielded 23.70 ± 0.50 g/L of xylose (237 mg/g of biomass) and 3.53 ± 0.17 g/L (35.3 mg/g of biomass) of glucose, whereas the raw biomass yielded 174 mg of xylose/g of biomass and 12.22 mg of glucose/g of biomass. Thus, the employment of DES pretreatment to yield more sugar from the holocellulose fraction is justified. In the second stage, the enzyme concoction (cellulase and xylanase) derived from *Aspergillus niger* was employed to the solid fraction obtained after mild acid hydrolysis. The enzymatic hydrolysate contained 239.1 mg of glucose/g of biomass and 24.5 mg of xylose/g of biomass, which is two-fold higher compared with the raw biomass, with resulting sugar yield of 141 mg/g and 11.43 mg/g of glucose and xylose, respectively. The hydrolysates derived from DES-pretreated biomass were further used for fermentation by *R. toruloides* to obtain value-added products such as xylitol and lipids. High hydrogen bond basicity is an important factor of an IL or DES that has been reported to be important for the dissolution of wood [63,64]. As the DES employed in this study was alkaline urea, this would have possibly enhanced the delignification followed by elevating the chance of enzyme accessibility on the exposed cellulose layer, thus the high yield of fermentable sugars compared to the raw biomass was obtained.

3.7. Co-Production of Xylitol and Lipids from Xylose by Free Cells of R. toruloides NCIM 3547

The xylose-rich hydrolysate derived from mild acid treatment was used for fermentation by *R. toruloides* to produce xylitol under microaerophilic conditions. Figure 4a shows the growth profile and xylose and glucose consumption (Figure 4b) by *R. toruloides*.

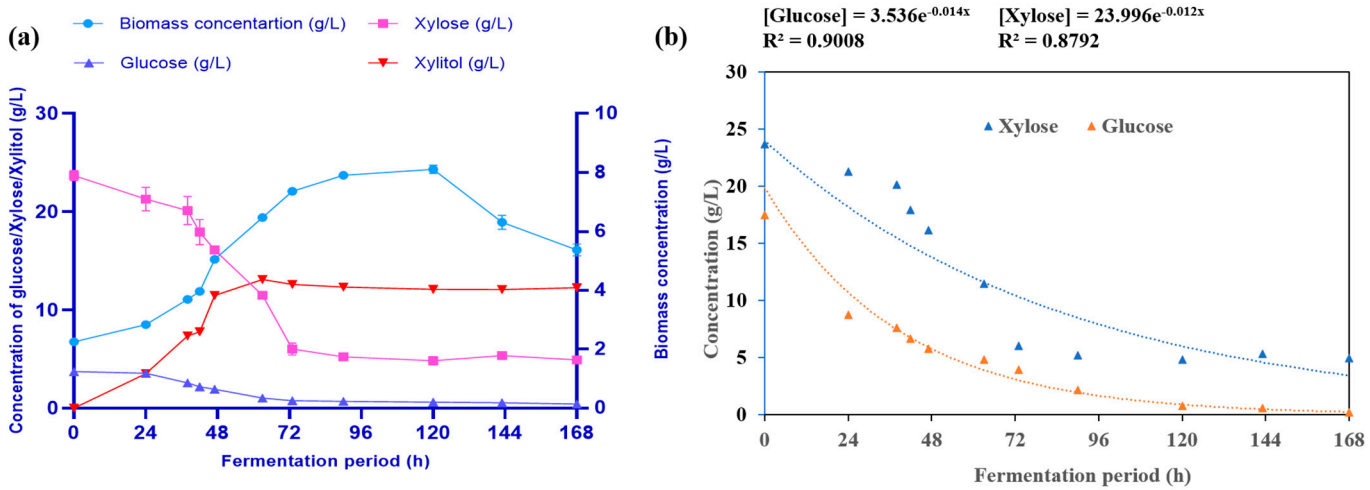

Figure 4. (**a**) Fermentation profile of hemicellulosic hydrolysate for xylitol production under microaerophilic free-cell conditions. (**b**) Substrate (glucose and xylose) consumption profile (based on first-order rate).

Supplementation of additional co-substrates such as glycerol and glucose were found to induce and enhance the xylitol production in yeasts [65,66]. As the WH hemicellulosic hydrolysate contains both xylose (23.07 g/L) and glucose (5.7 g/L), under microaerophilic conditions there is an exhibition of a diauxic growth pattern, as shown in Figure 4a. It has been observed that utilization of glucose was very rapid, which resulted in its consumption within 24 h, and was not repressed by xylose, which is higher compared with glucose. A similar observation was made in *Rhodotorula (Rhodosporidium) mucilaginosa*, in which the consumption of glucose was initiated rapidly (9 h) and not affected by the availability of xylose in a dual-sugar fermentation medium [67]. On the other hand, xylose consumption was somewhat repressed by the available glucose and rapid depletion of xylose occurred only after reduction of glucose to low levels. This observation was corroborated by our study in which the obtained sugar consumption rate for glucose and xylose resulted in 0.014 h^{-1} and 0.012 h^{-1}, respectively (Figure 4b and Table 4). It has been reported that in C5-utilizer yeast *Candida guilliermondii*, xylose consumption was repressed by glucose presence [68]. As represented by Figure 5, for xylitol production three main criteria need to be met to favour xylitol accumulation and efflux as follows: (i) presence of xylose (in excess compared with glucose) is required for upregulation of xylose reductase (XR) and xylitol dehydrogenase (XDH); (ii) minimizing the activity of XDH by increasing the NADH pool could favour the accumulation of xylitol and exert the efflux mechanism as demonstrated by Pinheiro et al. [16]; and (iii) reduced aeration (microaerophilic) with low volumetric oxygen transfer of 0.075 L/h, thereby routing the metabolism towards xylitol production rather than cell growth [69]. Hence, induced microaerophilic conditions were adopted in our study both at the head space and in the growth medium where an additional increase in xylose concentration could have favoured the xylitol synthesis that resulted in the yield of 4.37 g/L. From the fermentative parameters given in Table 4, the free-cell xylose fermentation resulted in a maximum specific growth rate (μ_m) of 0.075 h^{-1} with a product yield coefficient of 0.57 g of xylitol/g of xylose consumed, which is higher compared with the xylitol (0.3 g/g of xylose) obtained from *Rhodotorula (Rhodosporidium) mucilaginosa*. Upon comparing the biomass yield, the maximum biomass yield from our study is about 7.06 g/L, which is comparable to the reported yield of 7.8 g/L for *Rhodosporidium* sp [67].

Table 4. Kinetic parameters of different fermentations.

Parameters	Fermentation			
	Hemicellulosic Hydrolysate, Xylose-Rich Fraction	Cellulosic Hydrolysate, Glucose-Rich Fraction	Hemicellulosic Hydrolysate, Xylose-Rich Fraction in PBR	
			Cycle 1	Cycle 2
Maximum biomass yield (X_m), g/L (Based on Luedeking–Piret kinetic model)	7.06	10.98	-	-
Maximum specific growth rate (h^{-1}) (Based on Luedeking –Piret kinetic model)	0.075	0.20	-	-
Yield coefficient for biomass ($Y_{X/S}$) (g/g)	0.311	0.45	-	-
Yield coefficient for product ($Y_{P/S}$) (g/g)	0.57 (xylitol)	0.21 (lipid)	1.50 (xylitol)	1.80 (xylitol)
Rate of substrate consumption (q_s) g/L.h (Based on first-order kinetic model)	0.012	0.014	Xylose–0.84 Glucose–0.35	Xylose–0.95 Glucose–0.33
Rate of product formation (q_P) g/L.h	0.02	0.005	1.31	1.29
Substrate uptake efficiency	79.22% (xylose) 88.42% (glucose)	86.42% (glucose) 66.78% (xylose)	71.56% (xylose) 87.31% (glucose)	82.92% (xylose) 80.98% (glucose)

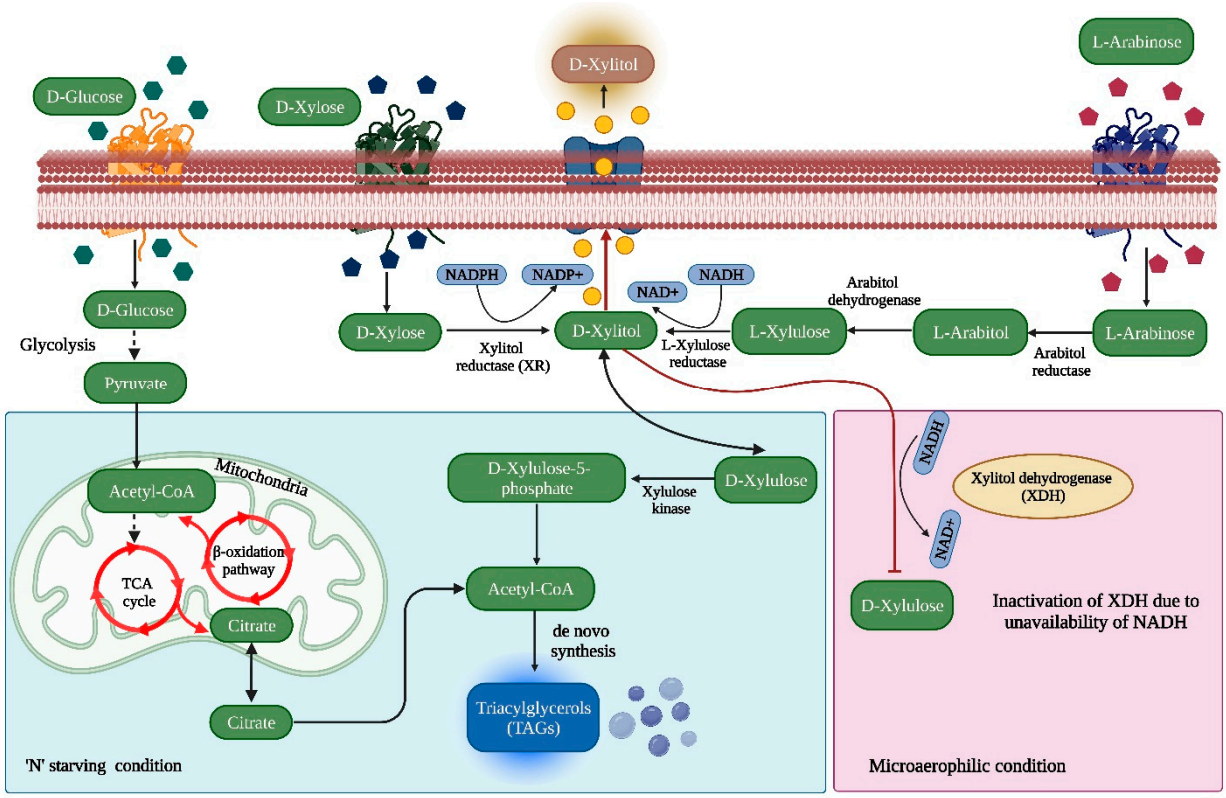

Figure 5. Proposed mechanism of selective uptake of sugars by Rhodosporidium toruloides through alteration of growth conditions (microaerophilic and 'N' limitation) for xylitol and lipid synthesis.

R. toruloides, the microbial candidate chosen for this study, is a well-known oleaginous yeast that exhibits a triauxic growth pattern in the presence of complex-waste-derived hydrolysates that consist of glucose, xylose and glycerol, which demonstrated the presence of different sugar transporters and their possible influx system during the growth cycle [29]. In general, *R. toruloides* prefers C6 as the primary carbon source; however, the use of other sources such as C5 sugars (xylose/arabinose) and glycerol has certain constraints mainly at metabolic levels. Therefore, the microbe needs either adaptation or modification at the genetic level. A conventional short- or long-term adaptation through ALE could be adopted as it is simple, cost effective and efficient for the microorganisms to adapt

with different compounds or conditions of interest [19]. The ALE method is based on phenotypic heterogeneity, not a genetic variation. In the case of a short-term adaptation, the transcriptional state of the most tolerant phenotype is inherited and prevails through the generations (transcriptional memory), which generates an epigenetic inheritance that might be a possible reason for the xylitol yield obtained in this study by selective utilization of xylose.

Consequently, the metabolic framework of *R. toruloides* is naturally segmented in such a way that it has the capability of synthesizing lipids from the consumed sugars (both C5 and C6 sugars) under 'N' limited conditions, which resulted in the final lipid content of 40.93%, *w/w*. These modulations during growth makes this yeast an ideal candidate for lipid and sugar alcohol production, as indicated in Figure 5, that postulates the possible metabolic route for diversified sugar utilization.

3.8. Production of Xylitol from Xylose by Immobilized R. toruloides NCIM 3547 in PBR

PBRs are used to carry out dynamic fermentation with the use of immobilized cells. Also, a PBR offers a higher conversion per weight of catalyst than other reactors with the advantage of reusing the immobilized cells. The conversion is based on the amount of the solid catalyst rather than the volume of the reactor.

Fermentation in the PBR as shown in Figure 6a was conducted using immobilized *R. toruloides* cells and xylitol yield was estimated. The xylose and glucose consumption by immobilized *R. toruloides* in cycle 1 and cycle 2 of the reactor studies is shown in Figure 6a. From the fermentation profile in Figure 6b, it can be observed that the trend in glucose and xylose uptake is same as that when using free cells. The maximum xylitol yield obtained from cycle 1 was observed to be 9.18 g/L and there was a slight decrease during the second cycle, with a yield of 8.99 g/L. However, considering the rate of substrate uptake based on the first-order kinetic model (Figure 6c) it was found that cycle 2 was better compared with cycle 1, which demonstrated the adaptation of the cells to the immobilized conditions and the reactor flow regime. Consequently, the yield coefficient of xylitol was found to be 1.5–1.8 g/g (Table 4), which is higher than for the free-cell system, which was 0.57 g/g. Rajeswari et al. [13] employed a PBR for production of ethanol from immobilized yeast using aloe vera leaf rind and compared its efficiency with the free-cell system. It has been reported that the PBR kinetic parameters were far better than the free-cell system in terms of substrate consumption rate, ethanol production rate and fermentation efficiency, which aligns the results of the PBR-based fermentation for xylitol production shown in Table 4. When compared with free cells, the immobilization of microbes can improve fermentation while lowering the total production cost. Immobilized cells become the noticeable and preferred alternative because they enable increased fermentation rates, cell reuse for extended period of time, protection of the entrapped cells from inhibitors and adverse environment, avoid washout, ease downstream processing of cells from the fermentation broth and reduced costs associated with inoculum development [69]. In this study, a xylitol yield comparable to that of free cells was obtained in both fermentation cycles using immobilized R.toruloides NCIM 3547 in a PBR, proving the above advantages.

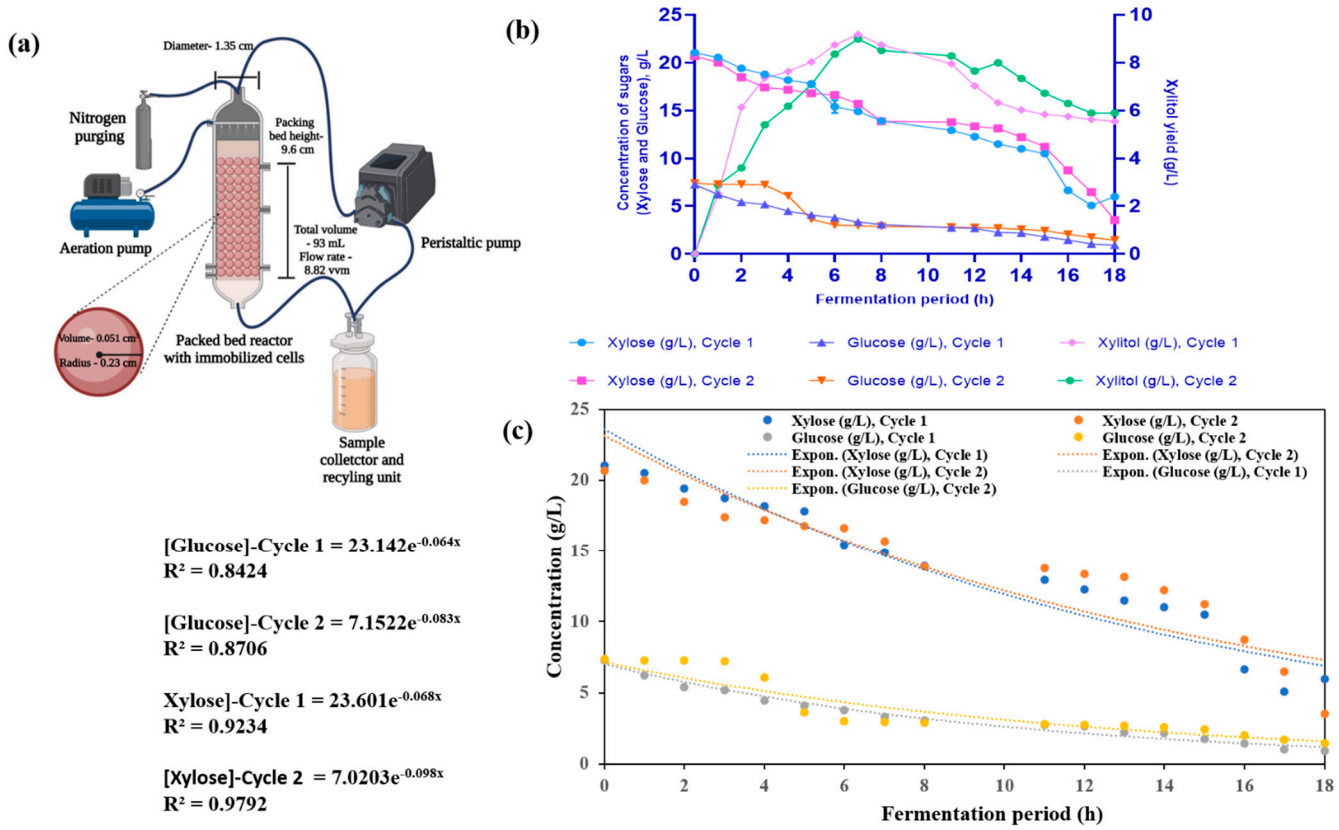

Figure 6. (**a**) Packed bed reactor (PBR) for immobilized cell-based fermentation. (**b**) Fermentation profile of hemicellulosic hydrolysate for xylitol production under microaerophilic immobilized-cell conditions. (**c**) Substrate (glucose and xylose) consumption profile (based on first-order rate).

3.9. Production of Lipids from Cellulosic Hydrolysate by R. toruloides

A surprising phenomenon to be noted in this strategy is that there is the possibility of lipid accumulation with the maintenance of a low N (nitrogen) level, thereby simultaneously producing the sugar alcohol and lipids through extracellular and intracellular mechanisms, respectively, as shown in Figure 7. Fillet et al. [70] reported that in *R. toruloides* NS-134 for improved lipid production, a C:N ratio of 20 is preferred. The hemicellulosic hydrolysate was used for lipid synthesis under 'N' limited conditions in which the supplementation of 3g/L yeast extract was replaced by 1.0 g/L of ammonium sulphate.

In our study, when WH-derived hydrolysate was employed as a 'C' source that had a C:N ratio of 24:1 in cellulosic hydrolysate it tended to yield lipids at about 46.81 ± 2.60%, (*w/w*) which is higher than the hemicellulosic hydrolysate that had a C:N ratio of 26.6:1, which yielded a lipid content of 40.93 ± 0.73% (*w/w*). Though, *R. toruloides* shows versatility in utilizing both glucose and xylose as a 'C' source, it is far less effective at producing them from xylose [70–72]. Consequently, the organisms require an extended period of fermentation for the production of lipids while utilizing xylose rather than glucose, which is evident from our study when employing hemicellulosic and cellulosic hydrolysates for lipid synthesis as indicated in Figure 7a–d. From Figure 7a, it has been observed that the glucose consumption increased from 24 h and then more rapidly up to 96 h, with a concomitant accumulation of lipids while growing. Compared with hemicellulosic hydrolysate, lipid content and the biomass yield were much higher under cellulosic hydrolysate fermentation (Figure 7b). Evidently, from Table 4 the substrate uptake efficiency in all modes of fermentation (free cells, hemicellulosic and cellulosic hydrolysate; immobilized hemicellulosic hydrolysate) were found to be predominant with glucose as compared to xylose.

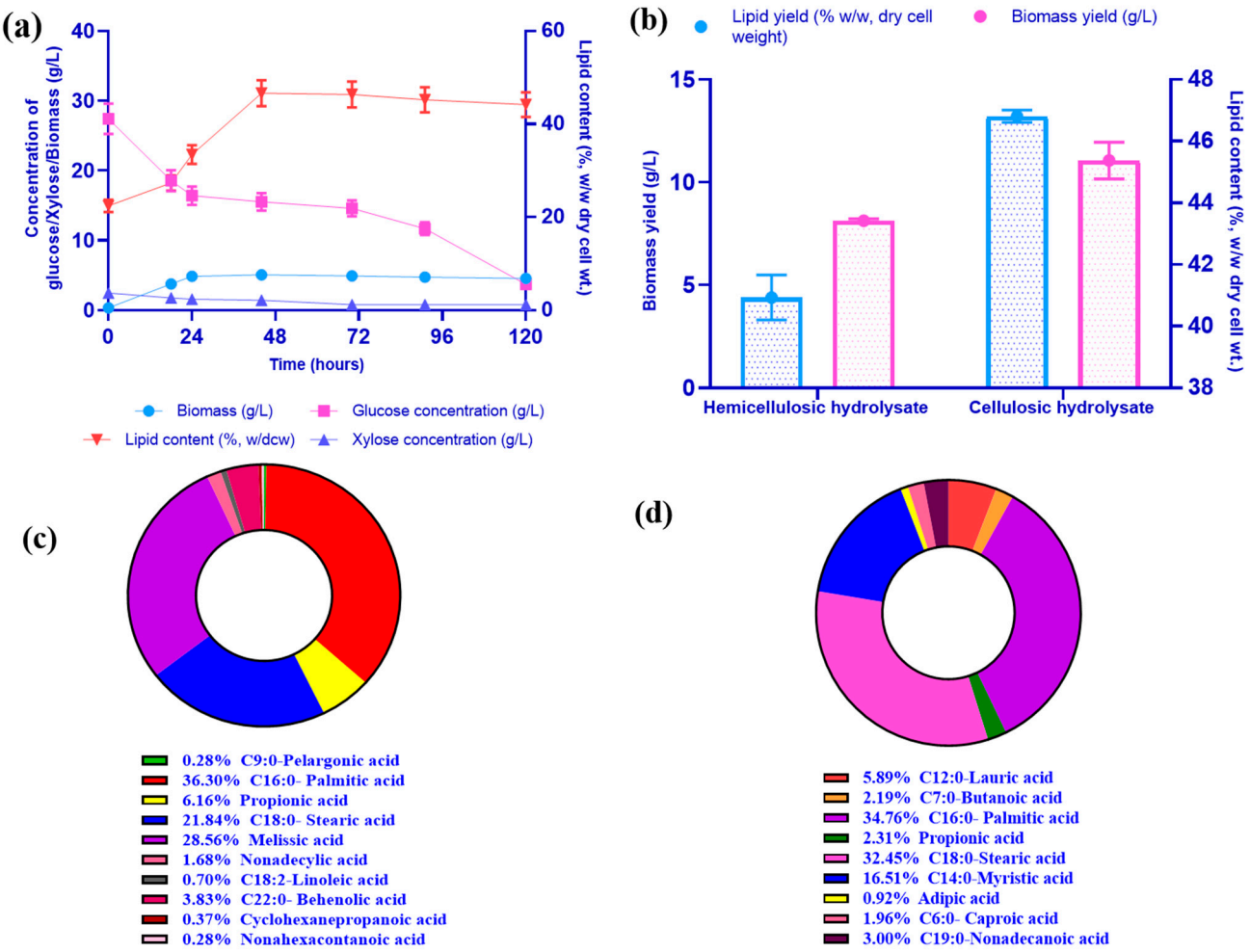

Figure 7. (**a**) Fermentation profile of cellulosic hydrolysate for lipid production under 'N' limitation conditions. (**b**) Comparison of lipid content and biomass yield between hemicellulosic and cellulosic hydrolysate. (**c**) FAME profile of lipids from hemicellulosic hydrolysate fermentation. (**d**) FAME profile of lipids from cellulosic hydrolysate fermentation.

However, by categorically utilizing the C5 and C6 sugar as a carbon source in different fermentations, a cumulative lipid content (46.81% + 40.93%, *w/w*) of around ~87% was obtained that exemplifies the strategic fermentation adopted in this study. Though the lipid production is prominent among yeasts cells under altered nutrient supplementation, it is also equally important to check the fatty acid composition of the accumulated lipid content for diversified applications such fuel (biodiesel) and pharmaceutical applications. The fatty acid composition of lipids depends upon the microbial strain and the cultivation conditions used [16]. Upon analysis of *R. toruloides*-NCIM-3547-derived lipids after transesterification for its FAME composition (Figure 7c,d), it was observed that the most common fatty acids are palmitic (C16:0), stearic (C18:0), oleic (C18:1) and linoleic (C18:2) acids, which is similar to the lipid fatty acid profile obtained from using both cellulosic and hemicellulosic hydrolysate where the combinatorial composition of C16:0 (palmitic) and C18:0 (stearic) constitute more than 50%, which seems to be analogous to common vegetable oil [70]. Therefore, these lipids could potentially replace vegetable lipids to produce biodiesel. An overall mass balance of the WH processing with DESs and the subsequent saccharification and fermentation adopted in this study has been presented in Supplementary Figure S7.

4. Conclusions

WH, an aquatic weed, was employed as feedstock for the co-production of xylitol (free cells—4.73 g/L; immobilized cells—9.18 g/L) and lipids (46.81% and 40.93%, *w/w*) by strategic fermentation of hemicellulosic and cellulosic hydrolysates using Rhodosporidium toruloides NCIM 3547. Additionally, a mild DES pretreatment using ChCl and urea was employed for the first time with the motive of extraction of lignin for its further application in value-added product production. Due to the techno-economic feasibility issues of second-generation biofuel production using LCB as a feedstock, there is a need for a paradigm shift from biofuel to biorefinery, i.e., single-feedstock-single-product to single-feedstock-multiproduct development. Also, biorefinery is not contextualised only on production of diversified products but also extent of utilization of all possible organic fractions that exist in LCB, namely, lignin, cellulose and hemicellulose through microbial valorization strategies with a sustainable framework. Hence, through this study successful hemicellulose and cellulose valorization routes with WH have been developed using a yeast biorefinery approach.

Supplementary Materials: The following supporting information can be downloaded at: https://www.mdpi.com/article/10.3390/fermentation8110591/s1, Figure S1: GPS image of the source of WH collected (Potheri: 12°49′03.6″ N 80°02′45.3″ E). The arrows indicate the infestation of the aquatic weed; Figure S2: HPLC chromatograms. (a) Standard xylitol. (b) Xylitol peak for Rhodosporidium toruloides NCIM 3547; Figure S3: Effect of (a) WH:DES ratio, (b) time and (c) temperature on percentage delignification (All the treatments were performed in triplicate and the values represent mean ± standard deviation); Figure S4: Standard plot for (a) xylose and (b) xylitol; Figure S5: FTIR spectra of (a) choline chloride, (b) urea and (c) choline chloride:urea; Figure S6: Residual plots for the optimization of WH pretreatment using DES through BBD-RSM; Figure S7: Mass flow of WH during pretreatment, saccharification (cellulose and hemicellulose) and fermentation for co-production of xylitol and lipids.

Author Contributions: Conceptualization, S.J. and V.K.; Methodology, S.J. and V.K.; Validation, S.J.; Formal Analysis, R.D.U., S.J. and V.K.; Investigation, R.D.U.; Data Curation, R.D.U.; Writing—Original Draft Preparation, R.D.U.; Writing—Review and Editing, S.J. and V.K.; Supervision, S.J. All authors have read and agreed to the published version of the manuscript.

Funding: This research received no external funding.

Institutional Review Board Statement: Not applicable.

Informed Consent Statement: Not applicable.

Data Availability Statement: The data presented in this study are available on request from the corresponding author. The data are not publicly available due to privacy.

Acknowledgments: The authors R.D.U and S.J., would like to acknowledge the Department of Biotechnology, School of Bioengineering, SRM Institute of Science and Technology, Kattankulathur for the financial and infrastructure support to carry out the research work. The authors would also like to acknowledge Nanotechnology Research Centre (NRC), and SRM Central Instrumentation Facility (SCIF), SRMIST for accessing the centralized instrumentation facility. V.K., would like to acknowledge the School of Water, Energy and Environment, Cranfield University, Cranfield, UK.

Conflicts of Interest: The authors declare no conflict of interest.

References

1. Vymazal, J. Constructed Wetlands, Surface Flow. In *Encyclopedia of Ecology*; Elsevier: Amsterdam, The Netherlands, 2008; pp. 765–776. ISBN 978-0-08-045405-4.
2. Pegg, J.; South, J.; Hill, J.E.; Durland-Donahou, A.; Weyl, O.L.F. Impacts of Alien Invasive Species on Large Wetlands. In *Fundamentals of Tropical Freshwater Wetlands*; Elsevier: Amsterdam, The Netherlands, 2022; pp. 487–516. ISBN 978-0-12-822362-8.
3. Wang, L.; D'Odorico, P. Decomposition and Mineralization. In *Encyclopedia of Ecology*; Elsevier: Amsterdam, The Netherlands, 2008; pp. 838–844. ISBN 978-0-08-045405-4.
4. Bai, F.; Chisholm, R.; Sang, W.; Dong, M. Spatial Risk Assessment of Alien Invasive Plants in China. *Environ. Sci. Technol.* **2013**, *47*, 7624–7632. [CrossRef] [PubMed]

5. Datta, A.; Maharaj, S.; Prabhu, G.N.; Bhowmik, D.; Marino, A.; Akbari, V.; Rupavatharam, S.; Sujeetha, J.A.R.P.; Anantrao, G.G.; Poduvattil, V.K.; et al. Monitoring the Spread of Water Hyacinth (Pontederia Crassipes): Challenges and Future Developments. *Front. Ecol. Evol.* **2021**, *9*, 631338. [CrossRef]
6. Verified Market Research. *Global Xylitol Market Size by Application (Chewing Gum, Confectionary, Food, Personal Care, Pharmaceuticals, Nutraceuticals), by Geographic Scope and Forecast*; Verified Market Research (VMR): Pune, India, 2021; p. 202.
7. Umai, D.; Kayalvizhi, R.; Kumar, V.; Jacob, S. Xylitol: Bioproduction and Applications—A Review. *Front. Sustain.* **2022**, *3*, 826190. [CrossRef]
8. Ahuja, V.; Macho, M.; Ewe, D.; Singh, M.; Saha, S.; Saurav, K. Biological and Pharmacological Potential of Xylitol: A Molecular Insight of Unique Metabolism. *Foods* **2020**, *9*, 1592. [CrossRef] [PubMed]
9. Wang, W.; Lee, D.-J. Lignocellulosic Biomass Pretreatment by Deep Eutectic Solvents on Lignin Extraction and Saccharification Enhancement: A Review. *Bioresour. Technol.* **2021**, *339*, 125587. [CrossRef]
10. Zdanowicz, M.; Wilpiszewska, K.; Spychaj, T. Deep Eutectic Solvents for Polysaccharides Processing. A Review. *Carbohydr. Polym.* **2018**, *200*, 361–380. [CrossRef]
11. Xu, H.; Kong, Y.; Peng, J.; Song, X.; Che, X.; Liu, S.; Tian, W. Multivariate Analysis of the Process of Deep Eutectic Solvent Pretreatment of Lignocellulosic Biomass. *Ind. Crops Prod.* **2020**, *150*, 112363. [CrossRef]
12. Massayev, S.; Lee, K.M. Evaluation of Deep Eutectic Solvent Pretreatment towards Efficacy of Enzymatic Saccharification Using Multivariate Analysis Techniques. *J. Clean. Prod.* **2022**, *360*, 132239. [CrossRef]
13. Rajeswari, G.; Arutselvy, B.; Jacob, S. Delignification of Aloe Vera Rind by Mild Acid Associated Microwave Pretreatment to Persuade Enhanced Enzymatic Saccharification. *Waste Biomass Valorization* **2020**, *11*, 5965–5975. [CrossRef]
14. Osorio-González, C.S.; Hegde, K.; Ferreira, P.; Brar, S.K.; Kermanshahipour, A.; Soccol, C.R.; Avalos-Ramírez, A. Lipid Production in Rhodosporidium toruloides Using C-6 and C-5 Wood Hydrolysate: A Comparative Study. *Biomass Bioenergy* **2019**, *130*, 105355. [CrossRef]
15. Pinheiro, M.J.; Bonturi, N.; Belouah, I.; Miranda, E.A.; Lahtvee, P.-J. Xylose Metabolism and the Effect of Oxidative Stress on Lipid and Carotenoid Production in Rhodotorula toruloides: Insights for Future Biorefinery. *Front. Bioeng. Biotechnol.* **2020**, *8*, 1008. [CrossRef] [PubMed]
16. Chattopadhyay, A.; Maiti, M.K. Lipid Production by Oleaginous Yeasts. In *Advances in Applied Microbiology*; Elsevier: Amsterdam, The Netherlands, 2021; Volume 116, pp. 1–98. ISBN 978-0-12-824594-1.
17. Manaf, S.F.A.; Luthfi, A.A.I.; Tan, J.P.; Abdul, P.M.; Jamali, N.S. Kinetic Study and Model of Fermentation Parameters Affected Growth and Xylitol Production in Bioreactor by Kluyveromyces marxianus ATCC 36,907. *Biomass Convers. Biorefin.* **2022**. [CrossRef]
18. Sasidharan, manekkara. EBird, Hotspot Report. Available online: https://ebird.org/hotspot/L3078680 (accessed on 25 September 2022).
19. Mavrommati, M.; Daskalaki, A.; Papanikolaou, S.; Aggelis, G. Adaptive Laboratory Evolution Principles and Applications in Industrial Biotechnology. *Biotechnol. Adv.* **2022**, *54*, 107795. [CrossRef] [PubMed]
20. Salimiyan, K.; Saberi, D. Choline Chloride/Urea as an Eco-Friendly Deep Eutectic Solvent for TCT-Mediated Amide Coupling at Room Temperature. *Chem. Select* **2019**, *4*, 3985–3989. [CrossRef]
21. Karlsson, H.; Ahlgren, S.; Sandgren, M.; Passoth, V.; Wallberg, O.; Hansson, P.-A. A Systems Analysis of Biodiesel Production from Wheat Straw Using Oleaginous Yeast: Process Design, Mass and Energy Balances. *Biotechnol. Biofuels* **2016**, *9*, 229. [CrossRef]
22. Procentese, A.; Johnson, E.; Orr, V.; Garruto Campanile, A.; Wood, J.A.; Marzocchella, A.; Rehmann, L. Deep Eutectic Solvent Pretreatment and Subsequent Saccharification of Corncob. *Bioresour. Technol.* **2015**, *192*, 31–36. [CrossRef]
23. Hussain, M.A.; Emdadul Hu, M.; Matiur Rah, S.; Ahmed, Z. Estimation of Lignin in Jute by Titration Method. *Pak. J. Biol. Sci.* **2002**, *5*, 521–522. [CrossRef]
24. Suopajärvi, T.; Ricci, P.; Karvonen, V.; Ottolina, G.; Liimatainen, H. Acidic and Alkaline Deep Eutectic Solvents in Delignification and Nanofibrillation of Corn Stalk, Wheat Straw, and Rapeseed Stem Residues. *Ind. Crops Prod.* **2020**, *145*, 111956. [CrossRef]
25. Segal, L.; Creely, J.J.; Martin, A.E.; Conrad, C.M. An Empirical Method for Estimating the Degree of Crystallinity of Native Cellulose Using the X-Ray Diffractometer. *Text. Res. J.* **1959**, *29*, 786–794. [CrossRef]
26. Narisetty, V.; Castro, E.; Durgapal, S.; Coulon, F.; Jacob, S.; Kumar, D.; Kumar Awasthi, M.; Kishore Pant, K.; Parameswaran, B.; Kumar, V. High Level Xylitol Production by Pichia fermentans Using Non-Detoxified Xylose-Rich Sugarcane Bagasse and Olive Pits Hydrolysates. *Bioresour. Technol.* **2021**, *342*, 126005. [CrossRef]
27. Miller, G.L. Use of Dinitrosalicylic Acid Reagent for Determination of Reducing Sugar. *Anal. Chem.* **1959**, *31*, 426–428. [CrossRef]
28. Pham, P.J.; Hernandez, R.; French, W.T.; Estill, B.G.; Mondala, A.H. A Spectrophotometric Method for Quantitative Determination of Xylose in Fermentation Medium. *Biomass Bioenergy* **2011**, *35*, 2814–2821. [CrossRef]
29. Singh, G.; Sinha, S.; Bandyopadhyay, K.K.; Lawrence, M.; Prasad, R.; Paul, D. Correction to: Triauxic Growth of an Oleaginous Red Yeast Rhodosporidium toruloides on Waste 'Extract' for Enhanced and Concomitant Lipid and B-carotene Production. *Microb. Cell Factories* **2019**, *18*, 37. [CrossRef] [PubMed]
30. Alankar, S.S.L.; Sajesh, N.; Rastogi, S.; Sakhuja, S.; Rajeswari, G.; Kumar, V.; Chandel, A.K.; Jacob, S. Bioprocessing of Fermentable Sugars Derived from Water Hyacinth into Microbial Lipids and Single Cell Proteins by Oleaginous Yeast Rhodosporidium toruloides NCIM 3547. *Biomass Convers. Biorefin.* **2021**. [CrossRef]
31. Sánchez, J. Colorimetric Assay of Alditols in Complex Biological Samples. *J. Agric. Food Chem.* **1998**, *46*, 157–160. [CrossRef]

32. Bligh, E.G.; Dyer, W.J. A Rapid Method of Total Lipid Extraction and Purification. *Can. J. Biochem. Physiol.* **1959**, *37*, 911–917. [CrossRef]
33. Xu, P. Analytical Solution for a Hybrid Logistic-Monod Cell Growth Model in Batch and Continuous Stirred Tank Reactor Culture. *Biotechnol. Bioeng.* **2020**, *117*, 873–878. [CrossRef]
34. Nigam, J.N. Bioconversion of Water-Hyacinth (*Eichhornia crassipes*) Hemicellulose Acid Hydrolysate to Motor Fuel Ethanol by Xylose–Fermenting Yeast. *J. Biotechnol.* **2002**, *97*, 107–116. [CrossRef]
35. Rathod, V.P.; Bhale, P.V.; Mehta, R.S.; Harmani, K.; Bilimoria, S.; Mahida, A.; Champaneri, H. Biogas Production from Water Hyacinth in the Batch Type Anaerobic Digester. *Mater. Today Proc.* **2018**, *5*, 23346–23350. [CrossRef]
36. Sindhu, R.; Binod, P.; Pandey, A.; Madhavan, A.; Alphonsa, J.A.; Vivek, N.; Gnansounou, E.; Castro, E.; Faraco, V. Water Hyacinth a Potential Source for Value Addition: An Overview. *Bioresour. Technol.* **2017**, *230*, 152–162. [CrossRef]
37. Feng, W.; Xiao, K.; Zhou, W.; Zhu, D.; Zhou, Y.; Yuan, Y.; Xiao, N.; Wan, X.; Hua, Y.; Zhao, J. Analysis of Utilization Technologies for *Eichhornia crassipes* Biomass Harvested after Restoration of Wastewater. *Bioresour. Technol.* **2017**, *223*, 287–295. [CrossRef] [PubMed]
38. Varanasi, J.L.; Kumari, S.; Das, D. Improvement of Energy Recovery from Water Hyacinth by Using Integrated System. *Int. J. Hydrog. Energy* **2018**, *43*, 1303–1318. [CrossRef]
39. Wauton, I.; Ogbeide, S.E. Characterization of Pyrolytic Bio-Oil from Water Hyacinth (*Eichhornia crassipes*) Pyrolysis in a Fixed Bed Reactor. *Biofuels* **2021**, *12*, 899–904. [CrossRef]
40. Sun, S.; Sun, S.; Cao, X.; Sun, R. The Role of Pretreatment in Improving the Enzymatic Hydrolysis of Lignocellulosic Materials. *Bioresour. Technol.* **2016**, *199*, 49–58. [CrossRef] [PubMed]
41. Chandel, A.K.; Garlapati, V.K.; Singh, A.K.; Antunes, F.A.F.; da Silva, S.S. The Path Forward for Lignocellulose Biorefineries: Bottlenecks, Solutions, and Perspective on Commercialization. *Bioresour. Technol.* **2018**, *264*, 370–381. [CrossRef] [PubMed]
42. Zhang, Q.; De Oliveira Vigier, K.; Royer, S.; Jérôme, F. Deep Eutectic Solvents: Syntheses, Properties and Applications. *Chem. Soc. Rev.* **2012**, *41*, 7108. [CrossRef]
43. Yadav, A.; Pandey, S. Densities and Viscosities of (Choline Chloride + Urea) Deep Eutectic Solvent and Its Aqueous Mixtures in the Temperature Range 293.15 K to 363.15 K. *J. Chem. Eng. Data* **2014**, *59*, 2221–2229. [CrossRef]
44. Shafie, M.H.; Yusof, R.; Gan, C.-Y. Synthesis of Citric Acid Monohydrate-Choline Chloride Based Deep Eutectic Solvents (DES) and Characterization of Their Physicochemical Properties. *J. Mol. Liq.* **2019**, *288*, 111081. [CrossRef]
45. Park, J.H.; Oh, K.W.; Choi, H.-M. Preparation and Characterization of Cotton Fabrics with Antibacterial Properties Treated by Crosslinkable Benzophenone Derivative in Choline Chloride-Based Deep Eutectic Solvents. *Cellulose* **2013**, *20*, 2101–2114. [CrossRef]
46. Wang, W.; Kong, Y.; Peng, J.; Li, B.; Xu, H. Probing the Mechanism of Green Solvent Solubilization of Hemicellulose Based on Molecular Dynamics Simulations. *Ind. Crops Prod.* **2022**, *186*, 115159. [CrossRef]
47. Smink, D.; Juan, A.; Schuur, B.; Kersten, S.R.A. Understanding the Role of Choline Chloride in Deep Eutectic Solvents Used for Biomass Delignification. *Ind. Eng. Chem. Res.* **2019**, *58*, 16348–16357. [CrossRef]
48. Hong, S.; Shen, X.-J.; Xue, Z.; Sun, Z.; Yuan, T.-Q. Structure–Function Relationships of Deep Eutectic Solvents for Lignin Extraction and Chemical Transformation. *Green Chem.* **2020**, *22*, 7219–7232. [CrossRef]
49. Sai, Y.W.; Lee, K.M. Enhanced Cellulase Accessibility Using Acid-Based Deep Eutectic Solvent in Pretreatment of Empty Fruit Bunches. *Cellulose* **2019**, *26*, 9517–9528. [CrossRef]
50. Wang, Z.-K.; Hong, S.; Wen, J.; Ma, C.-Y.; Tang, L.; Jiang, H.; Chen, J.-J.; Li, S.; Shen, X.-J.; Yuan, T.-Q. Lewis Acid-Facilitated Deep Eutectic Solvent (DES) Pretreatment for Producing High-Purity and Antioxidative Lignin. *ACS Sustain. Chem. Eng.* **2020**, *8*, 1050–1057. [CrossRef]
51. Mamilla, J.L.K.; Novak, U.; Grilc, M.; Likozar, B. Natural Deep Eutectic Solvents (DES) for Fractionation of Waste Lignocellulosic Biomass and Its Cascade Conversion to Value-Added Bio-Based Chemicals. *Biomass Bioenergy* **2019**, *120*, 417–425. [CrossRef]
52. Lee, K.M.; Quek, J.D.; Tey, W.Y.; Lim, S.; Kang, H.-S.; Quen, L.K.; Mahmood, W.A.W.; Jamaludin, S.I.S.; Teng, K.H.; Khoo, K.S. Biomass Valorization by Integrating Ultrasonication and Deep Eutectic Solvents: Delignification, Cellulose Digestibility and Solvent Reuse. *Biochem. Eng. J.* **2022**, *187*, 108587. [CrossRef]
53. Kalhor, P.; Ghandi, K. Deep Eutectic Solvents for Pretreatment, Extraction, and Catalysis of Biomass and Food Waste. *Molecules* **2019**, *24*, 4012. [CrossRef]
54. Zhang, P.P.; Tong, D.S.; Lin, C.X.; Yang, H.M.; Zhong, Z.K.; Yu, W.H.; Wang, H.; Zhou, C.H. Effects of Acid Treatments on Bamboo Cellulose Nanocrystals: Effects of Acid Treatments on Bamboo Cellulose Nanocrystals. *Asia-Pac. J. Chem. Eng.* **2014**, *9*, 686–695. [CrossRef]
55. Chi, X.; Liu, C.; Bi, Y.-H.; Yu, G.; Zhang, Y.; Wang, Z.; Li, B.; Cui, Q. A Clean and Effective Potassium Hydroxide Pretreatment of Corncob Residue for the Enhancement of Enzymatic Hydrolysis at High Solids Loading. *RSC Adv.* **2019**, *9*, 11558–11566. [CrossRef]
56. Piqueras, S.; Füchtner, S.; Rocha de Oliveira, R.; Gómez-Sánchez, A.; Jelavić, S.; Keplinger, T.; de Juan, A.; Thygesen, L.G. Understanding the Formation of Heartwood in Larch Using Synchrotron Infrared Imaging Combined with Multivariate Analysis and Atomic Force Microscope Infrared Spectroscopy. *Front. Plant Sci.* **2020**, *10*, 1701. [CrossRef]
57. Shi, Z.; Xu, G.; Deng, J.; Dong, M.; Murugadoss, V.; Liu, C.; Shao, Q.; Wu, S.; Guo, Z. Structural Characterization of Lignin from D. *sinicus by FTIR and NMR Techniques. Green Chem. Lett. Rev.* **2019**, *12*, 235–243. [CrossRef]

58. Subhedar, P.B.; Ray, P.; Gogate, P.R. Intensification of Delignification and Subsequent Hydrolysis for the Fermentable Sugar Production from Lignocellulosic Biomass Using Ultrasonic Irradiation. *Ultrason. Sonochem.* **2018**, *40*, 140–150. [CrossRef]
59. Chen, Y.; Mu, T. Application of Deep Eutectic Solvents in Biomass Pretreatment and Conversion. *Green Energy Environ.* **2019**, *4*, 95–115. [CrossRef]
60. Tian, D.; Chandra, R.P.; Lee, J.-S.; Lu, C.; Saddler, J.N. A Comparison of Various Lignin-Extraction Methods to Enhance the Accessibility and Ease of Enzymatic Hydrolysis of the Cellulosic Component of Steam-Pretreated Poplar. *Biotechnol. Biofuels* **2017**, *10*, 157. [CrossRef]
61. Fu, D.; Mazza, G. Aqueous Ionic Liquid Pretreatment of Straw. *Bioresour. Technol.* **2011**, *102*, 7008–7011. [CrossRef] [PubMed]
62. Wood, J.A.; Orr, V.C.A.; Luque, L.; Nagendra, V.; Berruti, F.; Rehmann, L. High-Throughput Screening of Inhibitory Compounds on Growth and Ethanol Production of Saccharomyces Cerevisiae. *BioEnergy Res.* **2015**, *8*, 423–430. [CrossRef]
63. Kilpeläinen, I.; Xie, H.; King, A.; Granstrom, M.; Heikkinen, S.; Argyropoulos, D.S. Dissolution of Wood in Ionic Liquids. *J. Agric. Food Chem.* **2007**, *55*, 9142–9148. [CrossRef] [PubMed]
64. Sun, N.; Rahman, M.; Qin, Y.; Maxim, M.L.; Rodríguez, H.; Rogers, R.D. Complete Dissolution and Partial Delignification of Wood in the Ionic Liquid 1-Ethyl-3-Methylimidazolium Acetate. *Green Chem.* **2009**, *11*, 646. [CrossRef]
65. Kogje, A.B.; Ghosalkar, A. Xylitol Production by Genetically Modified Industrial Strain of Saccharomyces cerevisiae Using Glycerol as Co-Substrate. *J. Ind. Microbiol. Biotechnol.* **2017**, *44*, 961–971. [CrossRef]
66. Ariyan, M.; Uthandi, S. Xylitol Production by Xylose Reductase over Producing Recombinant Escherichia coli M15. *Madras Agric. J.* **2019**, *106*, 205–209. [CrossRef]
67. Bura, R.; Vajzovic, A.; Doty, S.L. Novel Endophytic Yeast Rhodotorula mucilaginosa Strain PTD3 I: Production of Xylitol and Ethanol. *J. Ind. Microbiol. Biotechnol.* **2012**, *39*, 1003–1011. [CrossRef] [PubMed]
68. Zou, Y.; Qi, K.; Chen, X.; Miao, X.; Zhong, J.-J. Favorable Effect of Very Low Initial KLa Value on Xylitol Production from Xylose by a Self-Isolated Strain of Pichia guilliermondii. *J. Biosci. Bioeng.* **2010**, *109*, 149–152. [CrossRef] [PubMed]
69. Yewale, T.; Panchwagh, S.; Rajagopalan, S.; Dhamole, P.B.; Jain, R. Enhanced Xylitol Production Using Immobilized Candida tropicalis with Non-Detoxified Corn Cob Hemicellulosic Hydrolysate. *3 Biotech* **2016**, *6*, 75. [CrossRef]
70. Fillet, S.; Ronchel, C.; Callejo, C.; Fajardo, M.-J.; Moralejo, H.; Adrio, J.L. Engineering Rhodosporidium toruloides for the Production of Very Long-Chain Monounsaturated Fatty Acid-Rich Oils. *Appl. Microbiol. Biotechnol.* **2017**, *101*, 7271–7280. [CrossRef] [PubMed]
71. Jagtap, S.S.; Rao, C.V. Production of D-Arabitol from d-Xylose by the Oleaginous Yeast Rhodosporidium toruloides IFO0880. *Appl. Microbiol. Biotechnol.* **2018**, *102*, 143–151. [CrossRef]
72. Wei, N.; Quarterman, J.; Kim, S.R.; Cate, J.H.D.; Jin, Y.-S. Enhanced Biofuel Production through Coupled Acetic Acid and Xylose Consumption by Engineered Yeast. *Nat. Commun.* **2013**, *4*, 2580. [CrossRef]